

Free-breathing abdominal IVIM imaging

Yu-Chen TSAI¹ and Teng-Yi Huang¹

¹Department of Electrical Engineering, National Taiwan University of Science and Technology, Taipei, Taiwan

Target audience: MR physics working abdominal diffusion applications

Purpose

This study aims to apply intravoxel incoherent motion (IVIM) method to free-breathing abdominal imaging. We proposed a self-calibrating algorithm and a modified acquisition scheme to reduce image noise and artifacts caused by respiratory motion. This method was compared with the navigator-based method presented in previous studies.

Methods

Ten volunteers (8 men and 2 women, mean age: 23.3 yrs) participated in this study after obtaining informed consents. The IVIM experiments were performed on a 3T whole-body MR scanner (Tim Trio, Siemens) using a diffusion-weighted EPI sequence [TR/TE: 1500 / 78 ms, matrix size: 80 × 128, FOV: 187 × 300 mm, slice thickness: 5 mm, vector of diffusion gradient: (1, 0, 0), (0, 1, 0), (0, 0, 1)]. Ten transversal slices were acquired to cover liver and kidneys. Two acquisition schemes, M1 and M2 were performed. M1 was designed according to the study presented by Luciani A. et al.¹. In M1, 10 b values (0, 10, 20, 30, 40, 50, 100, 200, 400, 800 sec/mm²) were acquired with NEX of 3. The IVIM imaging sequence was respiratory-gated by using prospective adaptive navigator correction (PACE). In M2, 91 b values (initial: step: end, 0:5:200, 200:10:500, 500:20:800, 800:40:1000 sec/mm²) were acquired with NEX of 1. The acquisition of M2 is continuous without respiratory gating. Both M1 and M2 were repeated twice. The average scan time (n = 20, 10 subjects × 2 repeats) of M1 and M2 are 6.3 ± 1.2 min and 6.9 min, respectively. After experiments, we transferred the DICOM image files to a personal computer and performed data analysis using MATLAB® (Mathworks, Natick, MA, USA). For M1 data sets, the IVIM images underwent pixel-by-pixel curve fitting using Levenberg-Marquardt algorithm to estimate three parameters (f, D, D*) in IVIM model², given by $S_b/S_0 = (1 - f) \cdot \exp(-b \cdot D) + f \cdot \exp[-b(D + D^*)]$, where S_b is the signal intensity for each b value, S_0 is the signal intensity at a b value of zero, f is the fraction of the diffusion associated with microcirculation, D is related to pure molecular diffusion, and D* is the perfusion-related diffusion. The pixel-by-pixel fitting generated 3 maps (i.e., f, D and D* maps). The M2 data sets were acquired without respiratory-gating. Pixel misregistration caused by respiratory motion greatly hampers model-fitting accuracies. Thus, we proposed a two-step fitting procedure to reduce respiratory-related noise. First, the M2 data sets underwent pixel-by-pixel IVIM fitting with all 91 b values. The procedure calculated the fitting residuals of all pixels in each diffusion-weighted image and then determined a rejecting index (RI) by calculating the sum of the fitting residuals in the pixels in each image of the 91 diffusion-weighted images. Images with larger RI values were regarded as “bad” images which potentially induced noise in the fitting procedure. The next procedure selected amounts (e.g., 91, 81, 71, 61, 51) of images with the lowest RI and re-performed pixel-by-pixel IVIM model-fitting on the selected images to generate 3 maps of the IVIM model.

Results

Figure 1 displays D maps of the right kidney reconstructed from M1 and M2 data sets acquired from one of the subjects. The number denoted beneath each D map indicates the number of b values selected into IVIM-model fitting. Visual assessments of the D maps reveals that the kidney D map reconstructed using 71 b values (i.e., rejecting 20 b values) is the most homogeneous amount all the D maps. The standard deviations of the D and D* values in the kidney ROIs were calculated for each subject to assess spatial variations of D and D* values (σ_D and σ_{D^*}). Figure 2 displays the average σ_D and σ_{D^*} (n = 20, 10 subjects × 2 repeats) obtained using different number of b values. Selecting 61 values renders the lowest σ_D and selecting 71 values yields the σ_{D^*} comparable to that obtained using 10 b values (i.e., M1, respiratory-gated acquisition).

Discussion

This study developed a free-breathing abdominal IVIM imaging method. Previous studies acquired diffusion-weighted imaging with prospective respiratory gating multiple averages, and 10 b values. We proposed to acquire images with more b values and no averages (M1: 10 b values with NEX of 3, M2: 91 b values with NEX of 1). In the M2 data set, selecting all 91 b values into IVIM mapping very likely hampers the model-fitting because of respiratory motion. To deal with the potential artifacts, we used a retrospective selection algorithm based on rejecting indexes calculated from fitting residuals. The procedure selected 61 to 71 b values from 91 b values and reconstructed D and D* maps with prominently reduced spatial variations. Although the proposed M2 protocol acquires much more b values than the M1 protocol, the acquisition times of M1 and M2 are close (M1: 6.3 ± 1.2 min, M2: 6.9 min, n = 20). The σ_D obtained using M2 with the 61-b-value reconstruction was lower than that obtained using M1. The σ_{D^*} obtained using M2 with the 71-b-value was comparable to that obtained using M1. Compared to the M1 method, advantages of the M2 method are multi-fold. First, acquiring more b values in the M2 protocol allows rejecting images which introduces large fitting residuals. Secondly, the respiratory-gating used in M1 generally leads to an inconsistent repetition time between each DWI acquisition. The constant repetition time of the M2 protocol avoids two drawbacks in M1, the unpredictable scan times and inconsistent T1 recovery between each acquisition. A third point is that the free-breathing M2 method requires neither pneumatic bellow nor positioning the navigator echo. It could, therefore, potentially facilitate IVIM imaging in the clinical routine. A review article presented by Koh et al.³, suggested that a large number of b value would provide more data to estimate IVIM parameters. Lower b values (e.g., < 200 s/mm²) are especially critical to extract perfusion-sensitive information from DWI images. Thus, comparisons of reproducibility and accuracy of IVIM parameters obtained using M1 (10 b values with NEX of 3) and M2 (approximately 60 selected b values with NEX of 1) warrant further studies.

Conclusion

In conclusion, the proposed method, including the free-breathing acquisition scheme and the proposed reconstruction procedures provides a useful alternative to the navigator-gated methods. The free-breathing acquisition facilitates the setup procedures before scanning. Therefore, it could be a practical tool for abdominal IVIM imaging in the clinical environments.

Reference

1. Luciani A et al. Liver cirrhosis: intravoxel incoherent motion MR imaging—pilot study. Radiology 2008; 249:891–899.
2. Le Bihan D et al. Separation of diffusion and perfusion in intravoxel incoherent motion MR imaging. Radiology 1988; 168:497–505.
3. Koh DM et al. Intravoxel incoherent motion in body diffusion-weighted MRI: reality and challenges. Am J Roentgenol 2011; 196:1351–1361.

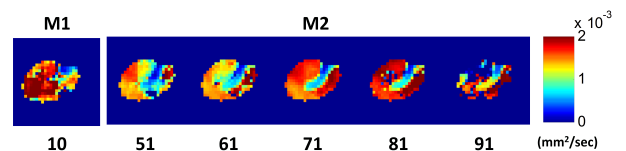


Figure 1: The right-kidney D maps acquired from one of the subjects. The number denoted beneath each D map indicates the number of b values selected into IVIM-model fitting. The acquisition times of DWI images were 6.8 min and 6.9 min for M1 and M2, respectively.

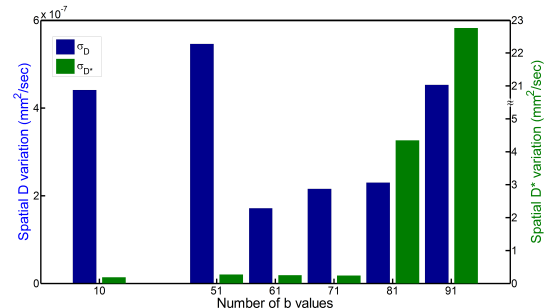


Figure 2: The average spatial variations, σ_D and σ_{D^*} obtained using different number of b values (n = 20, 10 subjects × 2 repeats). For M2, the optimal number of b values is approximately 60 to 70.